Human Molecular Genetics, 2007, Vol. 16, No. 10 ***1164–1175***
doi:10.1093/hmg/ddm064
Advance Access published on April 2, 2007

Modulation of nucleosome dynamics in Huntington's disease

Edward C. Stack[1,2], Steven J. Del Signore[2], Ruth Luthi-Carter[4,5], Byoung Y. Soh[2], Darlene R. Goldstein[4], Samantha Matson[2], Sarah Goodrich[2], Angela L. Markey[2], Kerry Cormier[1], Sean W. Hagerty[2], Karen Smith[1], Hoon Ryu[2] and Robert J. Ferrante[1,2,3,*]

[1]Geriatric Research Education and Clinical Center, Bedford VA Medical Center, 200 Springs Road, Bedford, MA 01730, USA, [2]Department of Neurology, [3]Department of Pathology and Psychiatry, Boston University School of Medicine, Boston, MA 02118, USA, [4]Mass General Institute of Neurodegenerative Disease, Building 114, 16th Street, Charlestown, MA 02129, USA and [5]Ecole Polytechnique Fédérale de Lausanne (EPFL), Lausanne CH-1015, Switzerland

Received January 26, 2007; Revised March 7, 2007; Accepted March 13, 2007

Transcriptional dysregulation and aberrant chromatin remodeling are central features in the pathology of Huntington's disease (HD). In order to more fully characterize these pathogenic events, an assessment of histone profiles and associated gene changes were performed in transgenic N171–82Q (82Q) and R6/2 HD mice. Analyses revealed significant chromatin modification, resulting in reduced histone acetylation with concomitant increased histone methylation, consistent with findings observed in HD patients. While there are no known interventions that ameliorate or arrest HD progression, DNA/RNA-binding anthracyclines may provide significant therapeutic potential by correcting pathological nucleosome changes and realigning transcription. Two such anthracyclines, chromomycin and mithramycin, improved altered nucleosome homeostasis in HD mice, normalizing the chromatin pattern. There was a significant shift in the balance between methylation and acetylation in treated HD mice to that found in wild-type mice, resulting in greater acetylation of histone H3 at lysine 9 and promoting gene transcription. Gene expression profiling in anthracycline-treated HD mice showed molecular changes that correlate with disease correction, such that a subset of downregulated genes were upregulated with anthracycline treatment. Improved nucleosomal dynamics were concurrent with a significant improvement in the behavioral and neuropathological phenotype observed in HD mice. These data show the ability of anthracycline compounds to rebalance epigenetic histone modification and, as such, may provide the rationale for the design of human clinical trials in HD patients.

INTRODUCTION

Huntington's disease (HD) is a fatal, autosomal dominant neurodegenerative disorder of mid-life onset, characterized by chorea, cognitive abnormalities and progressive dementia. The behavioral symptoms of HD are the consequence of a profound neurodegeneration, characterized by the primary involvement of the basal ganglia with substantial neuronal loss and concomitant astrogliosis (1). Underlying the behavioral and neuropathological sequela observed in HD is a genetic defect comprised of an expanded trinucleotide CAG repeat within the coding region of the *Huntingtin* gene on chromosome 4 (2). Normal huntingtin (Htt) is essential for embryogenesis (3), and is believed to play a role in vesicular transport (4). In addition, normal Htt may possess neuroprotective activity (5). In contrast, the trinucleotide expansion in mutant Htt (mHtt), which is thought to confer both a toxic gain-of-function in conjunction with a loss-of-function (6), is the arbiter of the neurodegeneration observed in HD (7).

While steady advances have been made over many years, the current understanding of disease pathogenesis has been greatly enhanced by the development of transgenic murine models of HD, which serve as valuable tools to study candidate disease mechanisms. The two most widely characterized

*To whom correspondence should be addressed at: Tel: +1 7816872908; Fax: +1 7816873515; Email: rjferr@bu.edu

HD mice are the N171–82Q (82Q) and R6/2 models (8,9). Both 82Q and R6/2 mice display progressive HD-like behavioral, biochemical and neuropathological alterations that parallel similar findings in HD patients (8–11). In addition, significant alterations in transcriptional activity mediated by mHtt have also been described in both 82Q and R6/2 mice (12–15).

One mechanism by which mHtt impacts transcription is through altered nucleosome dynamics. Important in this context, histone methylation and acetylation status is closely linked with transcriptional activity, regulating transcription factor access to promoter regions in DNA (16,17). Histone acetylation, which is generally regarded as promoting transcription, is reduced in models of HD (18,19). Conversely, histone methylation, which inhibits transcription, is increased in both 82Q and R6/2 mice (19,20). Histone methylation is also significantly elevated in HD patients (21). The disruption of transcriptional homeostasis through altered methylation and acetylation of histones and associated aberrant mHtt–protein interactions may trigger signaling cascades associated with a number of pathogenic mechanisms that can potentiate one another. Once activated, these signaling cascades may ultimately promote the neuronal dysfunction and subsequent cell death observed in HD. Conversely, drug agents that can realign chromatin homeostasis may improve HD-related deficits in transcription and thereby improve disease phenotype. To test this hypothesis, we administered chromomycin or mithramycin to HD mice and assessed their ability to correct aberrant nucleosomal dynamics and improve disease-related changes in transcription.

RESULTS

In order to assess the effects of anthracycline administration on nucleosome dynamics, western blot analyses of histone methylation and acetylation status were performed on brain samples from chromomycin-treated 82Q and R6/2 mice, as well as mithramycin-treated 82Q mice. Anthracycline treatment realigned chromatin homeostasis to that observed in wild-type (WT) mice. Untreated 82Q mice had significant hypoacetylation of H4, which was significantly improved by chromomycin (Fig. 1A; $F_{(2,18)} = 5.339$; $P < 0.02$). Mithramycin also significantly improved acetylation of histone H4 in 82Q mice [mean optical density (OD): WT, 0.436; 82Q untreated, 0.360; 82Q mithramycin, 0.465; $F_{(2,16)} = 4.965$; $P < 0.02$].

Concurrent analysis of methylation of histone H3 revealed significant increases in tri-methylation of H3 in untreated 82Q mice relative to WT controls (Fig. 1B; $F_{(3,22)} = 4.507$; $P < 0.02$). Chromomycin significantly reduced tri-methylation of H3 to levels indistinguishable from WT mice. Mithramycin also significantly improved methylation (mean OD: WT, 0.158; 82Q untreated, 0.232; 82Q mithramycin, 0.141; $F_{(2,15)} = 29.755$; $P < 0.01$). Similar results were observed in R6/2 mice. Analysis of acetylation of histone H4 showed significant hypoacetylation in R6/2 when compared with WT mice. Chromomycin administration significantly restored acetylation of histone H4 to WT levels (Fig. 1C; $F_{(3,22)} = 3.389$; $P < 0.05$). There was also a significant hypermethylation of histone H3 in untreated R6/2 mice when compared with WT littermate control mice (Fig. 1D) that was significantly reduced in chromomycin-treated R6/2 mice [$F_{(3,22)} = 7.059$; $P < 0.01$]. In addition, chromomycin treatment had no effect on total histone H3 levels in either 82Q or R6/2 mice (82Q—$F_{(2,15)} = 2.244$; $P > 0.05$; R6/2—$F_{(2,15)} = 0.850$; $P > 0.05$; data not shown).

As the methylation of histone H3 at lysine 9 is thought to be a dominant marker of transcription repression and since histone H3 can also be acetylated at lysine 9, the balance between methylation and acetylation of histone H3 at lysine 9 is believed to play an important role in the transcriptional disruption observed in HD (21). The ratio of methylation versus acetylation of histone H3 at lysine 9 in both 82Q and R6/2 mice showed significantly greater methylation when compared with WT mice (Fig. 2A and B). In contrast, chromomycin in 82Q and R6/2 mice, and mithramycin in 82Q mice, significantly shifted the tri-methyl/acetyl balance towards greater acetylation of histone H3 at lysine 9 [$F_{(2,15)} = 7.967$; $P < 0.01$; 82Q chromomycin: $F_{(3,22)} = 2.925$; $P < 0.05$; R6/2 chromomycin: $F_{(2,15)} = 21.387$; $P < 0.01$, 82Q mithramycin]. These findings demonstrate the ability of anthracyclines to alter nucleosomal dynamics, through modification of histone methylation and acetylation status, in a transcriptionally proactive manner.

We next assessed the impact of the correction of aberrant nucleosome status on mRNA levels in anthracycline-treated animals. A comparison of untreated R6/2 and WT mice showed a disease-related mRNA expression pattern in agreement with previous studies (12), with significant alterations observed in genes involved in neuronal signaling components, such as enkephalin, BDNF and the dopamine D2 receptor. Additional alterations in signal transduction, involving the transcription factor CREB, as well as mitogen-activated protein kinases, the cyclin-dependent kinase inhibitor 1A (P21) and the regulatory subunit 1B of protein phosphatase 1 are observed. Changes are also observed in gene expression involving products important to metabolism, such as glycerol-3-phosphate dehydrogenase 1. Such expression alterations correspond well with the metabolic dysfunction and impaired synaptic function observed in R6/2 mice (22,23).

Consistent with the predicted improvement in transcriptional status, mithramycin treatment ameliorated disease-related changes in mRNA levels observed in R6/2 mice. The main comparisons of interest are between mithramycin-treated R6/2 and saline-treated wild type mice, and between untreated R6/2 and wild type mice. In order to identify genes responding to drug treatment in the HD mice, we first restricted attention to genes differentially expressed between HD and wild type in the saline condition using a stringent threshold of B-stat > 0. We then identified which of these genes appear to be similarly expressed between HD drug-treated and wild type saline treated, using the criterion that the B-stat for this comparison should be < 0, indicating a drug-induced correction of a subset of aberrantly expressed genes. This subset of genes where expression is corrected by anthracycline treatment is represented graphically in the lower right quadrant of Figure 2C. HD-related mRNA changes were corrected by mithramycin treatment. While anthracycline-induced mRNA changes were not observed in

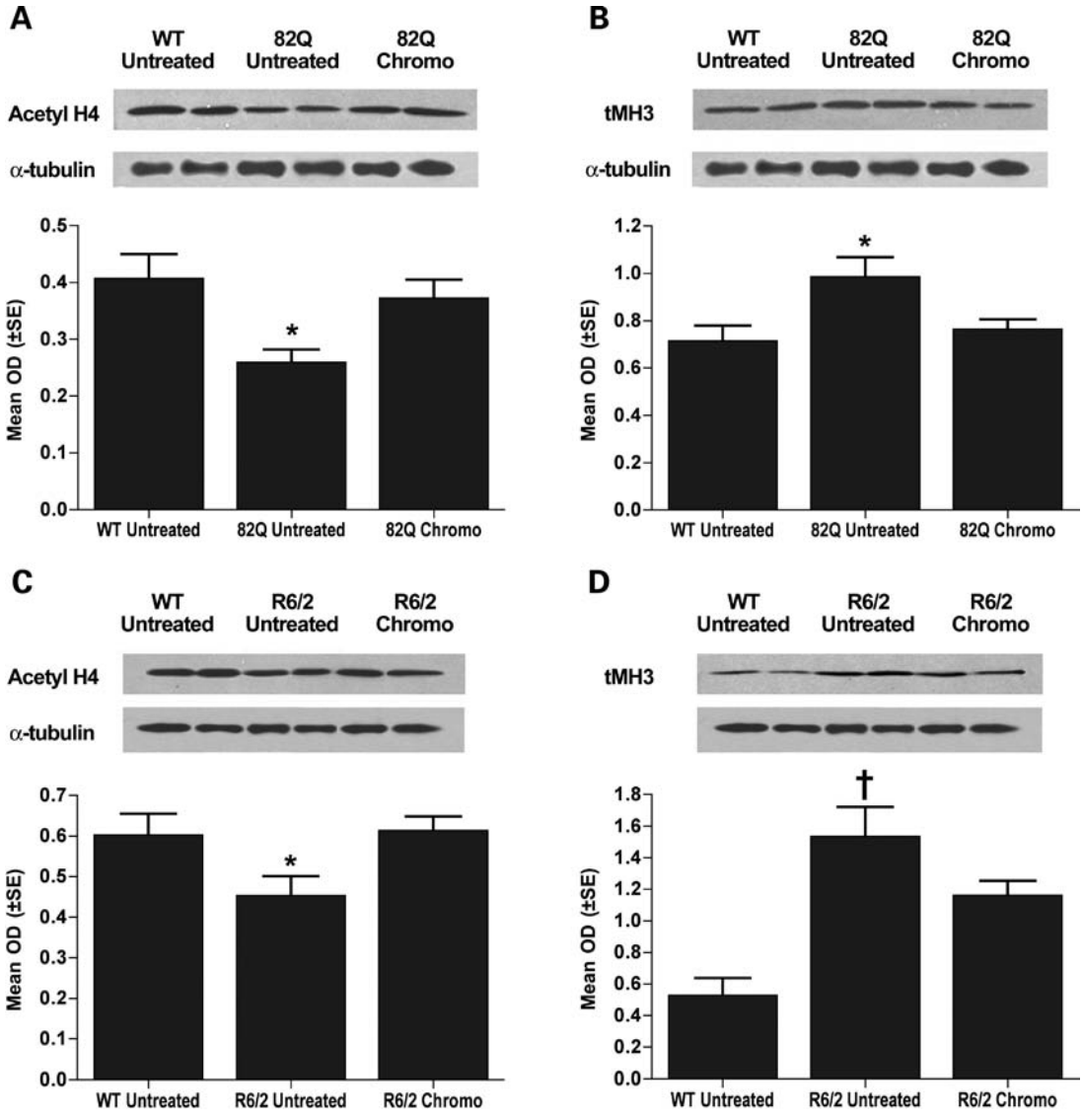

Figure 1. Histone methylation and acetylation alterations in chromomycin-treated 82Q and R6/2 mice. (**A**) 82Q mice exhibit significant hypoacetylation of histone H4 (AcH4) relative to WT mice at 120 days of age. Treatment with chromomycin (chromo) significantly improves acetylation of histone H4 in 82Q relative to untreated mice. (**B**) In contrast, 82Q mice demonstrate significant hypermethylation of histone H3 at lysine 9 (tMH3-K9). Chromomycin administration significantly improves methylation of histone H3 in 82Q mice. (**C**) R6/2 mice demonstrate significant hypoacetylation of histone H4 when compared with WT mice at 90 days. Chromomycin administration significantly improves acetylation of histone H4 in R6/2 such that they are indistinguishable from control mice. (**D**) R6/2 mice also exhibit a significant hypermethylation of histone H3 at lysine 9. Treatment with chromomycin significantly improves methylation of histone H3 in R6/2 mice. $^{*}P < 0.05$ versus untreated and chromo.

genes such as CREB or BDNF, mRNA's previously shown to be altered in R6/2 mice and demonstrating mithramycin-associated improvements in expression levels included the regulatory subunit 1B of protein phosphate 1 and the Ca^{++}/Calmodulin-dependent protein kinase I gamma, whose gene products are involved in regulating calcium homeostasis and signal transduction. A complete listing of mithramycin-induced improvements in gene expression levels can be found in Table 1.

Given the potential benefit on the overall HD phenotype conferred by the anthracycline-mediated improvement in nucleosomal dynamics, the effects of anthracycline administration on behavior and neuropathology were subsequently assessed in HD mice. Chromomycin significantly extended survival in 82Q mice by 25.5% in comparison with untreated mice (Fig. 3A; $\chi^2 = 18.92$; $P < 0.0001$; chromomycin: 168.1 ± 3.3 days; untreated: 134.0 ± 2.1 days). Mithramycin (100 μg) administration, which has previously been shown to be efficacious in R6/2 mice (20), also significantly increased survival in 82Q mice by 21.0% (Fig. 3A; $\chi^2 = 24.02$; $P < 0.0001$; mithramycin 161.9 ± 3.6 days). In addition, the most efficacious chromomycin dose (100 μg/kg) significantly increased survival in R6/2 mice by 13.1% (Fig. 3B; $\chi^2 = 14.11$; $P < 0.001$; chromomycin: 117.8 ± 5.7 days; untreated: 104.2 ± 1.9 days). Since there is evidence to suggest that exceeding total cumulative dose of

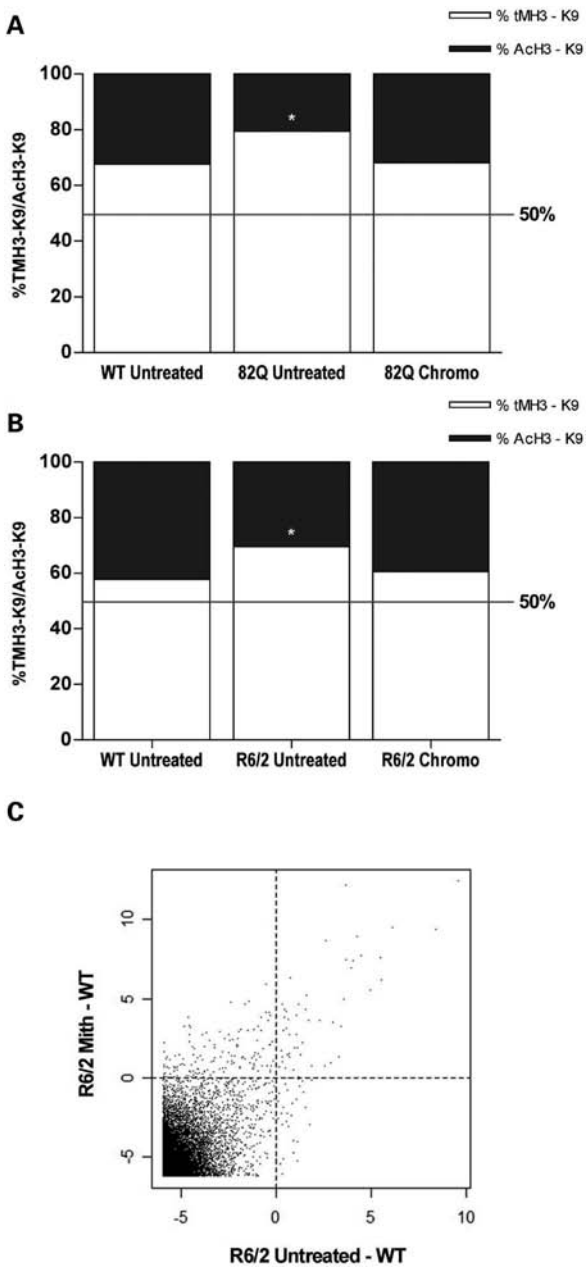

Figure 2. Histone H3 methylation versus acetylation balance in anthracycline treated 82Q and R6/2, and effect on mRNA expression. (**A**) Examination of the proportion of methylated H3 to acetylated H3 at lysine 9 (AcH3-K9) reveals a significant shift toward greater methylation in 82Q mice relative to WT control mice. In contrast, chromomycin (chromo) significantly shifts the balance toward greater acetylation of H3 at lysine 9. (**B**) Further examination of the relationship between methylated H3 and acetylated H3 at lysine 9 reveals a significant shift toward greater methylation in R6/2 mice relative to WT controls. In contrast, chromomycin significantly shifts the balance toward greater acetylation of H3 at lysine 9. (**C**) HD-related mRNA changes show correction of a subset of genes by anthracycline treatment. Plotted are individual gene B-statistics for the comparisons of mithramycin (mith)-treated R6/2 animals compared with WT animals (Y-axis) versus untreated R6/2 versus WT (X-axis). Dashed lines indicate the statistical cut-off, B-stat thresholds of 0 for each comparison. The genes for which expression is corrected toward WT by anthracycline treatment are indicated in the lower right quadrant of the scatter plot. $^{*}P < 0.05$ versus untreated and chromo.

mithramycin may result in toxicity, we introduced an intermittent dosing schedule that parallels chronic dosing in patients with HD. Interestingly, an intermittent mithramycin dosing schedule (400 μg/dose/week) significantly extended survival in R6/2 mice by 12.5% (R6/2 untreated, 104.5 days; R6/2 intermittent mithramycin, 117.0 days; $\chi^2 = 8.915$; $P < 0.01$).

While chromomycin and mithramycin significantly improve survival in 82Q mice, there was no effect observed on overall body weight loss (Fig. 3C). This was also true for R6/2 mice, where no significant effect on overall body weight loss was observed for chromomycin <100 μg (Fig. 3D). However, in mice receiving 200 μg of chromomycin, there was a significant weight loss observed between 54 [$F_{(4.60)}$, 7.910: $P < 0.01$] and 75 [$F_{(4.60)}$, 3.544; $P < 0.01$] days of age in R6/2 mice, suggesting toxicity at this dose (Fig. 3D). These findings are consistent with other compounds that remodel chromatin and provide transcriptional homeostasis in murine models of neurodegeneration (19–21).

An analysis of motor performance revealed significant differences between chromomycin-treated R6/2, untreated R6/2 and WT control mice in several measures of motor performance beginning at five weeks of age. Total ambulatory counts were significantly reduced in untreated R6/2 mice compared with WT mice at 5 weeks of age [$F_{(2,23)}$, 10.478; $P < 0.0006$] (Fig. 3E), and persisted through 14 weeks [$F_{(2,22)}$, 27.652; $P < 0.0001$]. Chromomycin significantly improved ambulation through 10 weeks [$F_{(2,22)}$, 6.876; $P < 0.0001$]. A similar pattern was observed for distance traveled (Fig. 3F). Untreated R6/2 mice traveled a significantly shorter distance when compared with WT mice at 7 weeks [$F_{(2,23)}$, 4.636; $P < 0.02$], through 14 weeks [$F_{(2,22)}$, 10.627; $P < 0.006$]. Treatment with chromomycin significantly increased distance traveled through 10 weeks [$F_{(2,22)}$, 8.391; $P < 0.01$]. Changes in locomotion were accompanied with an inverse pattern observed in resting time, where untreated R6/2 mice rested significantly more than WT mice beginning at 5 weeks of age [$F_{(2,23)}$, 4.452; $P < 0.02$] (Fig. 3G), and persisting through 14 weeks [$F_{(2,22)}$, 34.102; $P < 0.0001$]. Chromomycin treatment significantly reduced R6/2 resting time through 10 weeks of age [$F_{(2,23)}$, 34.102; $P < 0.0001$].

Anthracycline improvements in 82Q and R6/2 behavior likely result from an overall improved neuronal status. Supporting this view, chromomycin significantly abated the neuropathological sequela found in 82Q and R6/2 mice. Gross brain volume was significantly reduced in untreated 82Q mice when compared with WT mice (Fig. 4A). Striatal neuronal area was also significantly reduced in untreated 82Q compared with WT mice (Fig. 4B). Treatment with chromomycin or mithramycin (100 μg/kg, respectively) significantly improved gross brain volume in 82Q mice [Fig. 4C; $F_{(4,33)}$, 8.099; $P < 0.001$]. Anthracycline treatment also significantly improved striatal neuronal area, where greater efficacy was found in mithramycin-treated (67%) versus chromomycin-treated (36%) 82Q mice [Fig. 4D; $F_{(4,33)}$, 161.23; $P < 0.001$].

As in the 82Q mice, there was also a significant reduction in gross brain volume in untreated R6/2 mice when compared with WT mice (Fig. 5A). In keeping with these findings, there was a significant reduction in striatal neuronal area in

Table 1. Mithramycin treatment effects on gene expression in R6/2 cortex

ProbeSet ID	Gene name	Gene symbol	*B*-statistic	Log2-fold-change R6/2 saline versus WT saline	Log2-fold-change R3/2 treated versus WT saline
1423854_a_at	Ras-Like, family 11, member B	Rasl11b	1.8921	−0.8621	−0.4517
1426980_s_at	RIKEN cDDNA E130012A19 GENE	E130012A19Rik	1.75474	−0.8168	−0.4310
1424986_s_at	F-box and WD-40 domain protein 7, archipelago homolog (drosophila)	Fbxw7	1.5460	−0.5178	−0.3372
1459903_at	Semaphorin 7A	Sema7a	1.4292	−0.6536	−0.4922
1419225_at	Calcium chanel, voltage-dependent, alpha2/delta subunit 3	Cacna2d3	1.3726	−0.6453	−0.535
1448956_at	START domain containing 10	Stard10	1.2238	−0.3075	−0.2490
1418744_s_at	Tescalcin	Tesc	1.2014	−0.4808	−0.4114
1425895_at_at	Inhibitor of DNA binding 1	Idb1	1.1074	−0.3951	−0.1110
1421679_at_at	Cyclin-dependent kinase inhibitor 1A (p21)	Cdkn 1a	1.1067	−0.5278	−0.2343
1421992_atat	Insulin-like growth factor binding protein 4	Igfbp4	1.1028	−0.2935	−0.2150
1421926_at	Mitogen-activated protein kinase 11	Mapk 11	0.9429	−0.3673	−0.1711
1451331_at	Protein phosphatase 1, regulatory (inhibitor) subunit 1B	Ppp1r1b	0.9135	−0.5214	−0.1890
1417065_at	Unknown	–	0.8392	−0.7233	−0.5278
1424902_at	Plexin domain containing 1	Pldc 1	0.7910	−0.3604	−0.2365
1423007_a_at	Glial cell line derived neurotrophic factor family receptor alpha 2	Gfra2	0.6578	−0.4378	−0.2572
1424474_a_at	Calcium/calmodulin-dependent protein kinase kinase 2, beta	Camkk2	0.6487	−0.7719	−0.7079
1426562_at_at	Olfactomedin 1	Olfm 1	0.6045	−0.6501	−0.5493
1424480_s_at	Thymoma viral proto-oncogene 2	Akt2	0.5938	−0.3678	−0.2517
1417613_at	Immediate early response 5	Ier 5	0.5535	−0.7900	−0.4980
1416192_at	N-ethylmaleimide sensitive fusion protein attachment protein alpha	Napa	0.4749	−0.6227	−0.5573
1420596_at	Calcium channel, voltage-dependent, gamma subunit 2	Cacng2	0.3965	−0.3963	−0.1305
1423122_at	Arginine vasopressin-induced 1	Avpi 1	0.3709	−0.2772	−0.207
1415973_at	Myristoylated alanine-rich protein kinase C substrate	Marcks	0.3513	−0.2494	−0.0257
1420008_s_at	cDNA sequence BC07006	BC037006	0.3415	−0.4294	−0.2686
1421962_at	Unknown	–	0.2911	−0.3328	−0.2354
1423271_at	Gap junction membrane channel protein beta 2	Gjb2	0.2360	−0.2740	−0.0756
1448249_at	Glycerol-3-phosphate dehydrogenase 1 (soluble)	Gpd 1	0.1603	−0.3067	−0.2655
1426614_at	Protein kinase C binding protein 1	Prkcbp1	0.1334	−0.6535	−0.5285
1417071_s_at	Cytochrome p450, family 4, subfamily v, polypeptide 3	Cyp4v3	0.1306	−0.3433	−0.2343
1424633_at	Calcium/calmodulin-dependent protein kinase 1 gamma	Camk1g	0.0122	−0.2976	−0.2640

mRNA differentially expressed between R6/2 and wild-type mice (both saline-treated) for which drug treatment of R6/2 mice corrects expression to be more similar to wild-type, saline-treated mice.

untreated R6/2 mice when compared with WT mice (Fig. 5B). Chromomycin treatment (100 μg/kg) significantly improved gross brain atrophy [Fig. 5C; $F_{(2,10)}$, 8.418; $P < 0.01$], and the average striatal neuronal cell area in R6/2 mice [Fig. 5D; $F_{(2,10)}$, 183.09; $P < 0.001$].

The improvements in overall neuropathology were coincident with an improvement in the levels of oxidative damage. Urinary samples from 82Q mice showed significant elevations in urinary 8-hydroxy 2-deoxyguanosine (8-OH_2dG) in untreated mice when compared with WT mice [Fig. 6A; $F_{(2,26)} = 5.417$; $P < 0.01$]. There was a significant reduction in urinary 8-OH_2dG levels in chromomycin treated 82Q mice when compared with untreated 82Q mice. Additional analyses on brain 8-OH_2dG levels revealed significant anthracycline-mediated reductions. Brain 8-OH_2dG levels were elevated in both untreated 82Q and R6/2 mice [$F_{(3,32)} = 23.79$; $P < 0.01$; $F_{(2,19)} = 50.882$; $P < 0.01$; Fig. 6B and C, respectively]. Both human HD and R6/2 brain reveals significant oxidative DNA damage, demonstrated by elevations in 8-OH_2dG, associated with an impairment of oxidative phosphorylation within the basal ganglia (24,25). Chromomycin treatment in 82Q and R6/2 mice, and mithramycin treatment in 82Q mice, significantly reduce brain 8-OH_2dG levels.

DISCUSSION

Chromatin structure in eukaryotic cells is a dynamic, yet highly regulated process that occurs through interactions between DNA and histone proteins. These interactions influence efficient chromosomal packaging. Assemblies of core histone proteins form an octamer around which DNA can wind, resulting in distinct histone/DNA conformations: condensed heterochromatin, with its compact nature tending towards transcriptional silencing (26), or the more relaxed euchromatin, a relatively open region of chromatin associated with transcriptional activity (27). The associations of histone proteins with DNA can be altered by epigenetic histone modifications to influence transcription (16).

Among the more prominent modifications of histone proteins H3 and H4, methylation and acetylation play a significant role in transcriptional activity (16,17,26,28). Histone acetylation is regulated through the concerted actions of histone acetyltransferases (HAT) and histone deacetylases (HDACs) (26). It is widely held that HAT activity results in increased DNA transcription (29). In contrast, histone deacetylation mediated by HDAC activity, is associated with transcriptional repression (27). Additional chromatin remodeling is also mediated through the activity of histone

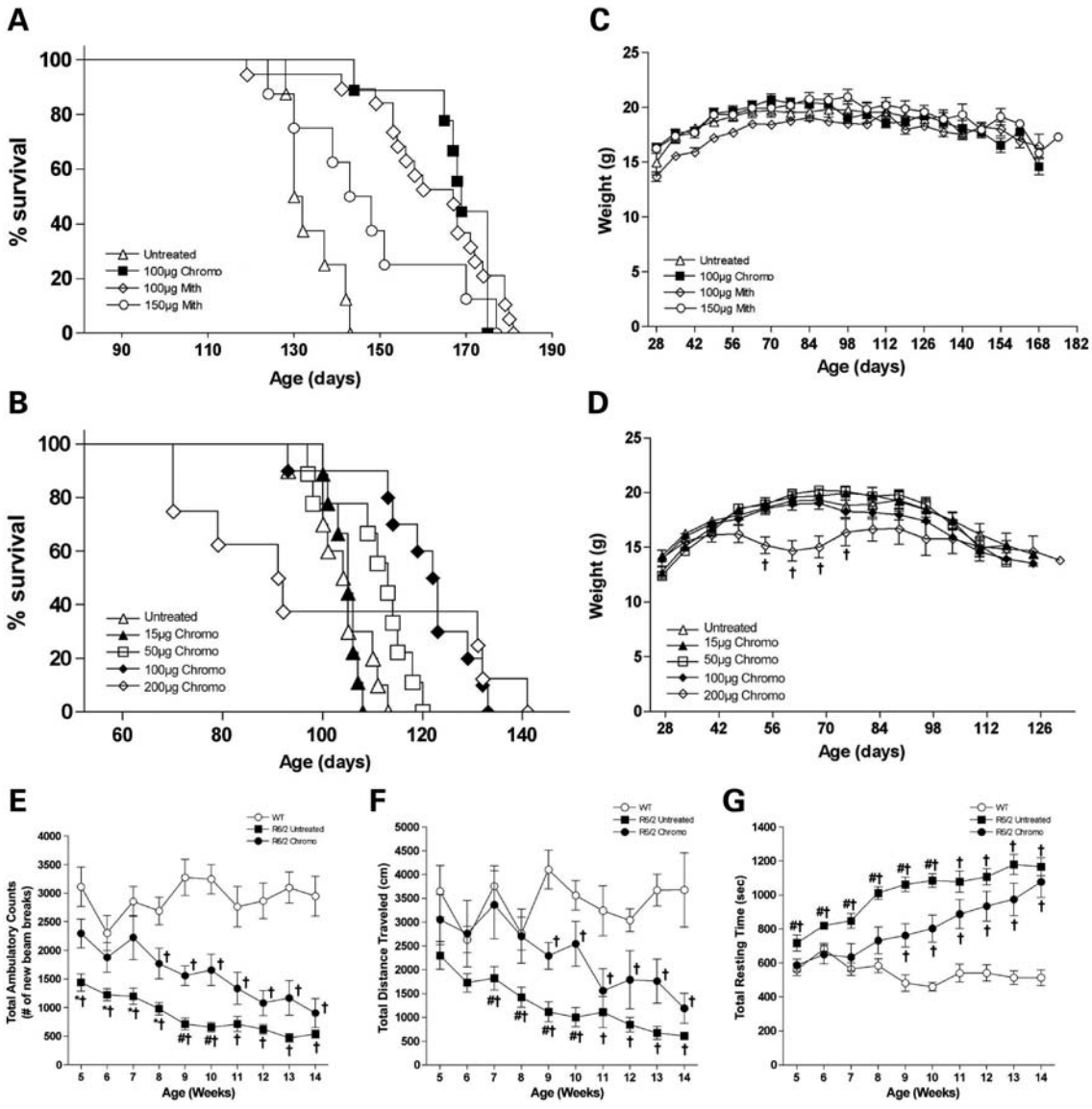

Figure 3. The effects of anthracycline administration on survival, body weight and locomotor behavior in 82Q and R6/2 mice. (**A**) 82Q mice received 100 μg/kg of chromomycin (chromo, closed squares), 100 μg/kg mithramycin (mith, open diamonds) or 150 μg/kg mithramycin (open circles), in comparison with untreated 82Q control mice (open triangles), all anthracycline treatments significantly extended survival in 82Q mice (100 μg/kg chromomycin, 25.4%; 100 μg/kg mithramycin, 21.0%; 150 μg/kg mithramycin, 10.3%). (**B**) R6/2 mice received either 15 (closed triangles), 50 (open squares), 100 (closed diamonds) or 200 μg/kg (open diamonds) of chromomycin. Additional R6/2 mice were untreated (open triangles). Doses of 50 and 100 μg of chromomycin significantly improved R6/2 survival by 5.8 and 13.1%, respectively. (**C**) 82Q mice treated with either 100 μg/kg chromomycin, 100 or 150 μg/kg mithramycin did not differ in body weight from untreated 82Q mice at any time point examined. (**D**) R6/2 mice treated with 15, 50 or 100 μg/kg chromomycin demonstrated no significant differences in body weight with WT mice at any time point examined. In contrast, R6/2 mice treated with 200 μg/kg chromomycin were significantly different from all other groups between 54 and 68 days. (**E**) WT control mice (open circles) demonstrate significant elevations in total ambulatory counts, defined as the total number of new beam breaks, over untreated R6/2 mice (closed squares). Chromomycin significantly improves total ambulatory counts in R6/2 mice (closed circles). (**F**) Similar to above, R6/2 untreated mice demonstrate significant reductions in total distance traveled, with WT mice demonstrating significant increases relative to untreated R6/2 mice. Chromomycin significantly improves R6/2 performance. (**G**) In contrast, R6/2 untreated mice demonstrate significant increases in resting time compared to WT mice. Chromomycin significantly reduces R6/2 resting time. $^{**}P < 0.01$ versus Untreated; $^{*}P < 0.05$ versus Chromo; $\#P < 0.01$ versus Chromo; $\dagger P < 0.01$ versus WT.

methytransferases, the actions of which may have profound implications on transcriptional repression. Methylation of H3 at lysine 9, in particular, is thought to promote gene silencing (30), although recent data suggests that the position of methylated histones along the entire gene can have an influence over gene silencing versus transcription (31).

Changes in chromatin structure are a prominent pathological feature of many neurodegenerative diseases. In Alzheimer's disease (AD), aberrant processing of the amyloid precursor protein results in significant transcriptional alterations (32,33). In keeping, altered gene transcription in AD has recently been associated with alterations in histone

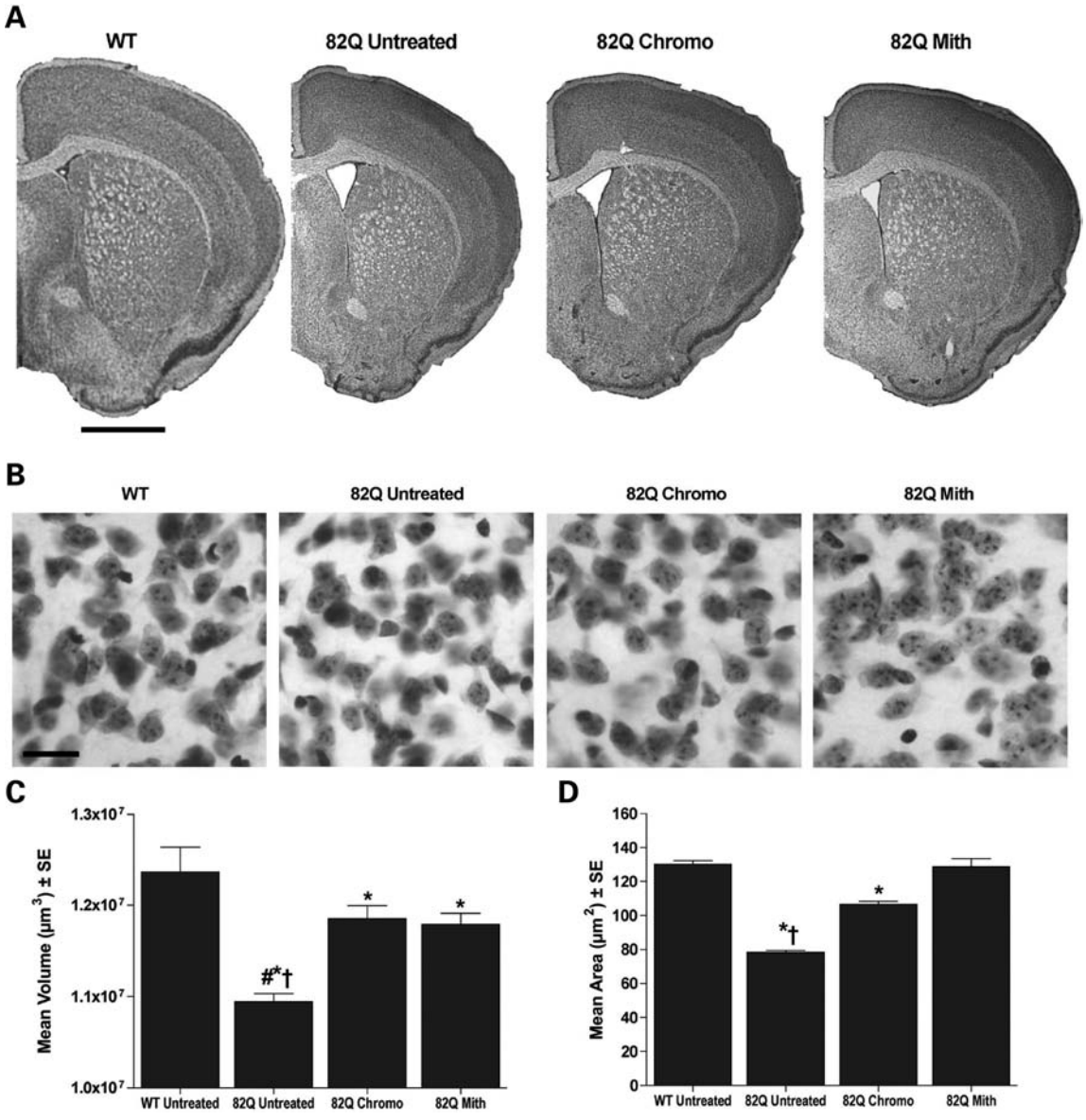

Figure 4. Effects of anthracycline administration on 82Q brain morphology. (**A**) Gross brain volume is reduced in 82Q mice compared with WT control mice, and a significant improvement is observed after either chromomycin (chromo) or mithramycin (mith) treatment. (**B**) 82Q mice also demonstrate a significant decrease in striatal neuronal area when compare to WT control mice. (**C**) Chromomycin (100 μg/kg) and mithramycin (100 μg/kg) significantly improve brain volume in 82Q mice. (**D**) Again, both chromomycin (100 μg/kg) and mithramycin (100 μg/kg) significantly improves average striatal neuronal area in 82Q mice compared to untreated mice. $^{*}P < 0.01$ versus WT-untreated; †$P < 0.01$ versus 82Q Chromo; # $P < 0.01$ *v.* 82Q Mith.

acetylation profiles (34). Transcriptional anomalies are also observed in Parkinson's disease, where a subset of genes identified in expression profiling studies are significantly dysregulated (35). In both cases, neuropathogenic alterations in transcriptional activity lead to perturbations in normal neuronal function and neuronal death. However, the association between neuronal death and transcriptional dysfunction is no more evident than in HD.

A profound aspect of disease pathology in HD is a significant reduction in gene transcription (15,36,37). One molecular basis for transcriptional dysregulation is likely to be the result of direct interactions between the mHtt protein and several transcription factors (38–41), which occur early in disease. Interestingly, transcriptionally active anthracyclines and HDAC inhibitors can improve transcription profiles in murine models of HD (18–20). The mechanism by which these compounds offer benefit is likely the result of epigenetic modifications of the histone–DNA complex.

Experimental studies have linked significant hypoacetylation of H4 in murine models of HD (18–20), and in human HD (unpublished data). As well, hypermethylation of H3 is also linked to human HD patients and HD mice (20,21). These epigenetic modifications of histone proteins in HD likely promote alterations in chromatin packaging that results in transcriptional

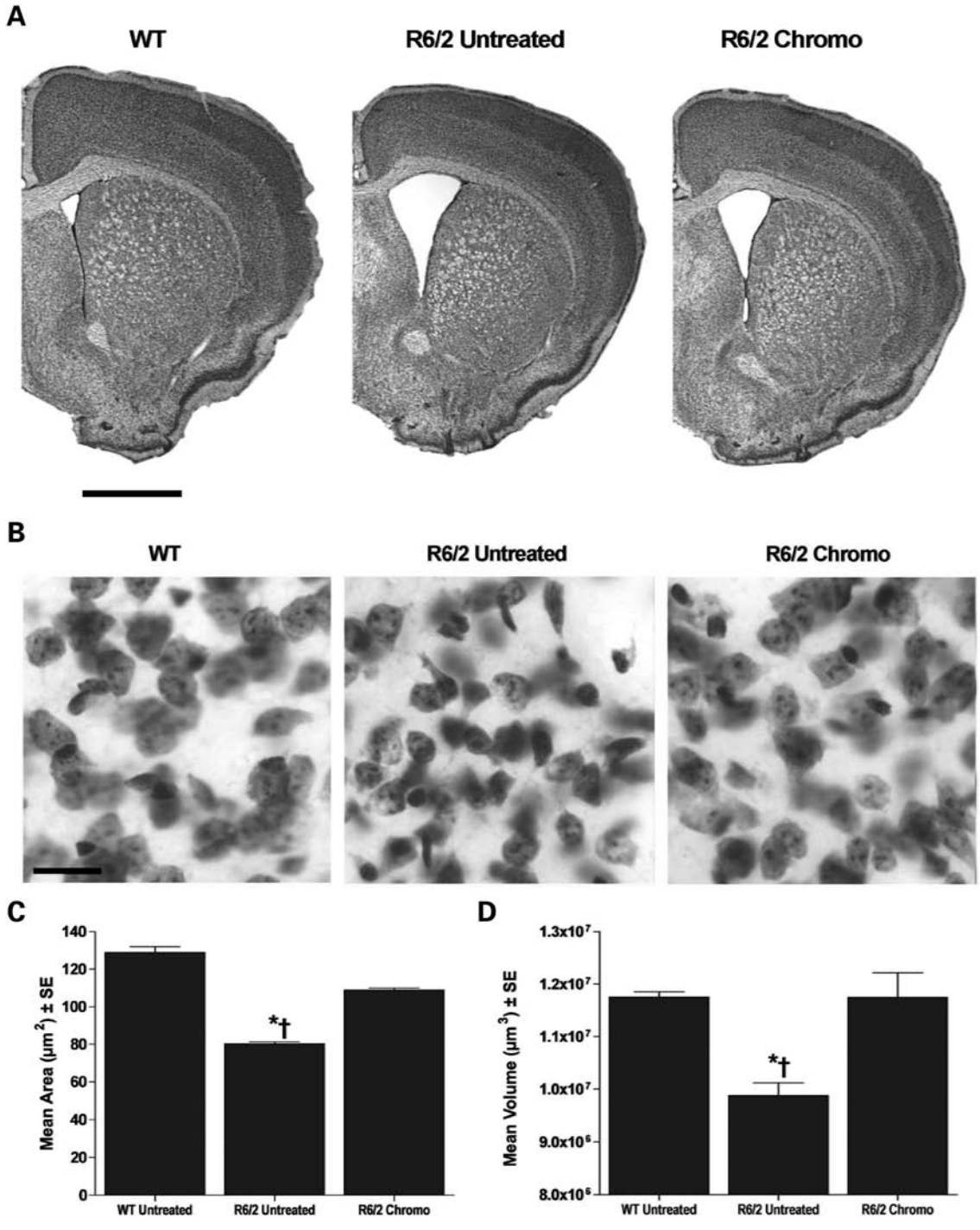

Figure 5. Effects of anthracycline administration on R6/2 brain morphology. (**A**) Photomicrograph demonstrating the significant reduction in brain volume of R6/2 when compared with WT control mice, with the improvement observed after chromomycin (chromo) treatment. (**B**) There is also a significant reduction in striatal neuronal area in R6/2 when compared with WT mice, and the improvement after chromomycin administration (**C**) Chromomycin (100 μg/kg) significantly improves brain volume in R6/2 mice. (**D**) In addition, chromomycin (100 μg/kg) significantly improves average striatal neuronal area in R6/2 mice. $^{*}P < 0.01$ versus WT-untreated; †$P < 0.01$ versus R6/2 Chromo.

repression. Compounds that can realign histone homeostasis can exert neuroprotective effects. The anthracycline antibiotics chromomycin and mithramycin are two clinically approved DNA-binding drugs that are similar in structure and mechanism of action. Chromomycin belongs to a class of aureolic acid group antibiotics and is produced by *Streptomyces griseus* (42). Mithramycin is produced by *Streptomyces argillaceus*. The anti-tumor properties of mithramycin and chromomycin

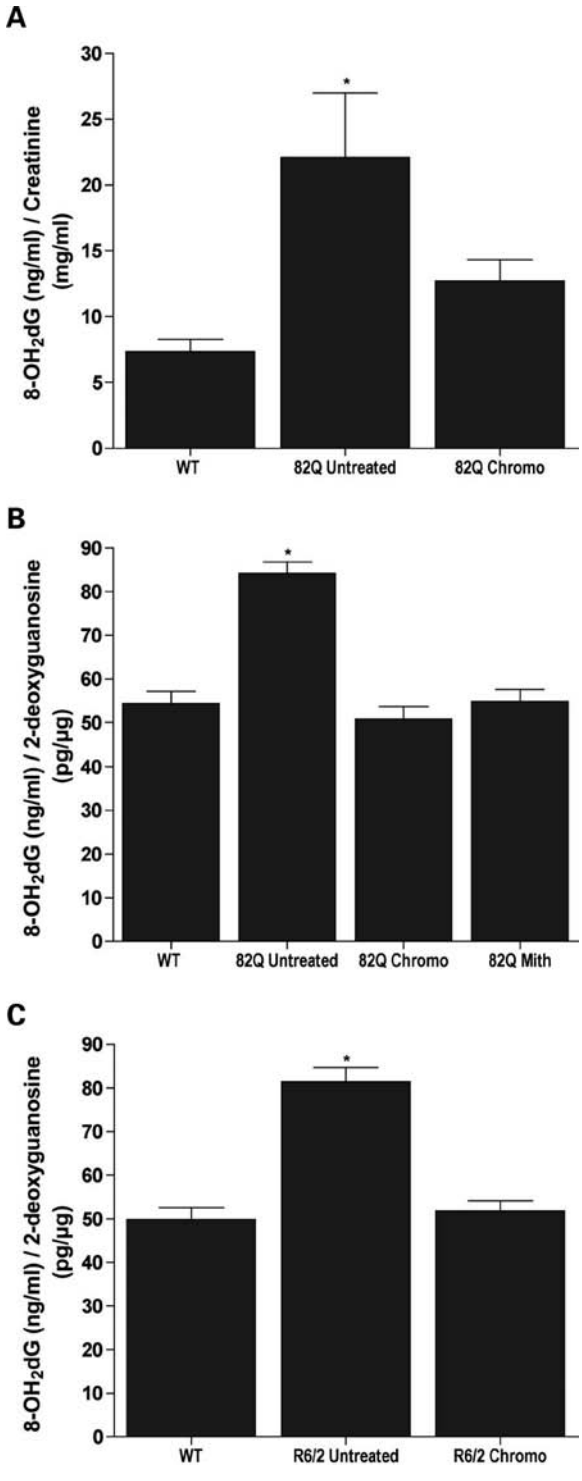

Figure 6. The effects of anthracycline administration on urinary and brain 8-OH_2dG levels in 82Q and R6/2 mice. (**A**) Urinary 8-OH_2dG levels are significantly elevated in 82Q mice relative to WT mice. Chromomycin (chromo) treatment significantly reduces 8-OH_2dG levels in 82Q mice, indistinguishable from WT mice. (**B**) A similar pattern is observed in brain 8-OH_2dG levels. Brain 8-OH_2dG levels are significantly elevated in 82Q mice relative to WT controls. Either chromomycin or mithramycin (mith) treatment significantly reduces 8-OH_2dG levels in 82Q mice, indistinguishable from WT mice. (**C**) A similar pattern of significantly elevated brain 8-OH_2dG is also observed in R6/2 mice. Treatment with chromomycin significantly reduces 8-OH_2dG levels in R6/2 mice. $^*P < 0.01$ versus WT-untreated.

are ascribed to their inhibitory effects on replication and the transcription process. They act by selectively modulating gene expression/transcription by displacing transcription activators and repressors that bind to guanine–cytosine-rich regions of promoters (43–45). Anthracycline compounds have also been demonstrated to interact directly with core histone proteins H3 and H4 (46).

It may seem paradoxical that cytostatic or cytotoxic medications may have a role in neurodegenerative disorders. While parallels between oncogenesis and neurodegenerative disorders have been suggested, cellular stresses and transcriptional signals elicit different responses in cells that enter the cell cycle versus cells that are terminally differentiated, leading to oncogenesis in the former, and neurodegeneration in the latter. Stressed neurons respond transcriptionally by turning genes on and off in compensation, with subsequent triggering of genetic programs executing cell death. Compensatory genetic responses, as well as cell death, might also be incompletely performed due to transcriptional dysregulation (47). Thus, neurons may become even more vulnerable to generic stress for which they cannot compensate and, at the same time, may not be able to fully execute apoptosis. This would explain why degenerating neurons (in humans and transgenic mice) seem to persist for so long without expressing a clear apoptotic phenotype.

Altered histone methylation and acetylation are consistent with reduced transcriptional activity as related to the 'histone code' (30,48). Administration of chromomycin or mithramycin significantly shifts the balance of methylation versus acetylation of histone H3 at lysine 9 towards greater acetylation. In turn, this promotes a transcriptionally proactive chromatin packaging (29). As such, anthracyclines can promote a return to neuronal homeostasis that results in significant neuroprotection. Of principal importance, these therapeutic agents promote significant proactive changes in nucleosomal dynamics that counteract the pathogenic disruptions in transcriptional activity.

Both mithramycin and chromomycin have been used as cancer chemotherapeutics. Mithramycin's greatest use in cancer was for testicular malignancy, although it is now rarely used because of improved therapeutics for testicular cancer. At lower doses, mithramycin is a very effective inhibitor of osteoclastic activity, and has been used with good safety, tolerability and efficacy in Paget's disease and hypocalcaemia of malignancy until it was supplanted by biphosphates (43,49–51). Interesting, mitoxantrone, another DNA-binding antibiotic similar to mithramycin, has been effectively used in progressive multiple sclerosis (52). While mithramycin and chromomycin have not been used chronically and may have dose-related toxicity in humans (53), the present preclinical mouse studies provide a rationale for the pursuit of safety and tolerability trials using anthracycline compounds in HD patients.

MATERIALS AND METHODS

Animals

Transgenic male 82Q and R6/2 mice from stable established colonies maintained at the Bedford facility were bred with females from their background strain (B6 CBAFI/J). The

progeny were genotyped via PCR assay on DNA isolated from tail biopsy. The length of the CAG repeat was monitored by the Core Sequencing Facility at Boston University. A total of 90 transgenic female mice and 30 WT control female mice were employed for experiments involving 82Q mice. Experiments involving R6/2 mice required a total of 110 transgene positive female mice and 30 littermate WT control female mice. All mice of the same 'F' generation were weighed at 20 days of age and equally distributed according to parentage and weight within each group to ensure homogeneity of each experimental cohort. Mice under 8 g at this time point were not used in the experiments. All mice were housed five per cage under standard conditions with *ad libitum* access to food and water. Enrichment conditions were not applied to any cages. The mice were handled under the same conditions by one investigator at the same time of the day. All animal experiments were performed in accordance with the NIH Guide for the Care and Use of Laboratory Animals and were approved by both the Veterans Administration and Boston University Animal Care Committees.

Drug administration

R6/2 mice ($N = 10$/group) received daily intraperitoneal (i.p.) injection with chromomycin (vehicle, 15, 50, 100, 200, 400 and 600 μg/kg: SERVA Electrophoresis, Heidelberg, Germany) dissolved in normal saline (0.9%)/ethanol (0.0005%). 82Q mice ($N = 10$/group) received daily i.p. injections of chromomycin (vehicle, 100 μg/kg). Additional 82Q mice ($N = 10$) received daily i.p. injections with mithramycin (100, 150 μg/kg; SERVA Electrophoresis, Heidelberg, Germany) dissolved in normal saline (0.9%). The initial dosing paradigm of 150 μg/kg mithramycin in 82Q mice was chosen based on previous use of mithramycin in R6/2 mice (20). However, this dose proved to be less efficacious in extending survival, likely as a consequence of toxicity from prolonged administration of mithramycin. There is evidence to support that mithramycin may result in cardiomyopathy when the total cumulative dose is exceeded (53). All treatment paradigms began at 28 days of age and included a group of untreated WT. Injection volumes for all mice were 100 μl. Animals used for microarray studies received 150 μg/kg/day of mithramycin.

Microarray gene expression profiling

Total RNA of 10 μg from the cerebral cortices of individual animals were processed using the Affymetrix GeneChip One-Cycle Amplification kit and corresponding cRNA probes were hybridized to MOE430A arrays. Quality of chip hybridization images was assessed with the RMA-QC approach (54) implemented in the BioConductor R package affyPLM. In this method, gene expression is modeled as the sum of chip and probe effects, with the model fit by robust regression (i.e. outliers are downweighted). Pseudoimages of the robust regression weights or residuals for each probe provide a graphical means to assess chip quality; numerical measures indicative of quality were also computed. By these criteria, all chips were of similar and suitably high quality that none required exclusion.

Survival

All mice were observed twice daily to monitor general feeding capability and motor performance. Criteria for euthanasia was the point in time when mice could no longer right themselves after 30 s when positioned on their side and gently prodded. This was confirmed by two separate observers (E.C.S. and R.J.F.) and considered the time of death. A limited number of deaths occurred overnight, and the time of death was recorded as the following morning.

Motor performance and body weight

An Opto-Varimax Auto-Track System (Columbus Instruments, Columbus, OH, USA) was used to assess motor performance of R6/2 chromomycin-treated mice. Beginning at 35 days of age, chromomycin-treated (100 μg/kg) and -untreated transgenic mice ($N = 10$/group) and WT ($N = 10$) mice were evaluated weekly on the same day and time. Mice were placed in a clean, clear polycarbonate cage measuring 29 cm × 18.5 cm × 12.5 cm. The cage was positioned inside the horizontal sensor of the Opto-Varimax detector array. The position of the cage in the array was kept constant throughout testing. Any beam interruption is recorded and processed by the Auto-Track System (ATS) software. The ATS software recorded three separate measures: total ambulatory counts, total resting time and total distance traveled. Body weights were obtained once a week at the same day and time.

Histological evaluation

Chromomycin-treated (100 μg/kg) and -untreated 82Q ($N = 10$/group) and R6/2 ($N = 10$/group), mithramycin-treated (100 μg/kg) 82Q ($N = 10$) mice, and WT ($N = 10$) mice were deeply anesthetized and transcardially perfused with 4% buffered paraformaldehyde at 120 days of age for 82Q mice and 90 days of age for R6/2 mice. The brains were removed, post-fixed in the perfusate for 2 h, rinsed in buffer and cryoprotected in a graded series of 10 and 20% glycerol/2% dimethyl sulfoxide. Frozen serial sections were cut at 50μm, stored in 6-well plates and stained for Nissl substance using cresyl violet. Tissue sections were examined using a Nikon Eclipse E800 microscope with a Spot RT digital camera.

Stereology and quantitation

Coronal-cut serial sections from the rostral segment of the neostriatum to the level of the anterior commissure (interaural 5.34 mM/bregma 1.54 mM to interaural 3.7 mM/bregma 0.10 mM) (55) were used for all volumetric and striatal neuron analyses. Striatal neuronal areas and striatal and ventricular volumes were analyzed by microscopic video capture and analyzed using ImageJ (56).

Western blot analysis

Brains from chromomycin-treated (100 μg/kg) and -untreated 82Q and R6/2 mice ($N = 10$/group), mithramycin-treated (100 μg/kg) and -untreated 82Q ($N = 10$/group) and WT ($N = 20$) mice were processed for western blot analysis. The 82Q and R6/2 mice were euthanized at 120 and 90 days,

respectively, and brains were flash frozen and stored at −80°C. Histone methylation and acetylation was determined by western blot analysis as previously reported (18,20). Frontal cortex was homogenized, processed for histone isolation and total protein concentration was determined using a DC assay kit (Bio-Rad, Hercules, CA, USA). Samples were then subjected to SDS–PAGE (10%) and probed for tMH3 (1:3000, Upstate, Charlottesville, VA, USA), AcH3 (1:1500; Upstate) or AcH4 (1:2000; Upstate). Protein loading was controlled for by subsequently assessing alpha-tubulin (1:5000; Upstate) on the same membrane. Quantification of tMH3, AcH3, AcH4 and alpha-tubulin was performed by densitometric analysis using NIH Image J (56).

High-performance liquid chromatography analysis

Urine samples were collected from 82Q mice ($N = 9$/group) at 120 days of age and analyzed by HPLC for the detection of free 8-OH_2dG. Urine was collected in 1.5 ml tubes and diluted 1:1 with 8% MeOH, 0.1 M lithium acetate, pH 6.4. The dilution buffer dissolves particulates that co-precipitate with 8-OH_2dG. Samples were stored at −80°C. 8-OH_2dG was detected using a liquid chromatographic electrochemical carbon column switching technique (57). Final 8-OH_2dG concentration (ng/μg) was determined by the relative ratio of 8-OH_2dG/creatinine. Brain samples from 82Q mice ($N = 9$/group) and R6/2 mice ($N = 7$/group) were also analyzed for the detection of 8-OH_2dG (10). Samples were stored at −80°C. The supernatant of each sample (10 μL) was separated using the liquid chromatographic electrochemical carbon column switching technique, as noted above. Standards for 8-OH_2dG were prepared in buffers used for sample preparation, respectively, to accurately determine peak identity.

Statistics

Interval scale data involving only two independent groups were analyzed using the *t*-test. Interval scale data involving more than two groups were analyzed using one-way analysis of variance. If an overall significant difference was detected, multiple comparisons were performed with Fishers least significant difference test. For all analyses, a significance level of $P \leq 0.05$ was observed. Statistical analyses of gene expression measures were carried out with open source R software packages available as part of the BioConductor project (http://www.bioconductor.org). Gene expression was quantified by robust multi-array analysis (58,59) using the affy package (60). To identify genes differentially expressed between conditions for each brain region, we computed single gene B-statistics (61) using the limma package (62).

ACKNOWLEDGEMENTS

Thanks to Ayshe Beesen, Affymetrix GeneChip Core at the Harvard Medical School Biopolymers Facility. H.R. and R.J.F. are grant awardees of the Jerry McDonald Huntington's Disease Foundation from Boston University School of Medicine. Supported by NIH NS52724-01 (H.R.), NIH NS045242 (R.J.F. AND RL-C), NS045806 (R.J.F.), the High Q Foundation and the Huntington's Disease Society of America (H.R. and R.J.F.), the EPFL (RL-C) and the Veterans Administration (R.J.F.).

Conflict of Interest statement. The authors have had no involvements that might raise the question of bias in the work reported or in the conclusions, implications or opinions stated.

REFERENCES

1. Hersch, S.M., Rosas, H.R. and Ferrante, R.J. (2004) Neuropathology and pathophysiology of Huntington's disease. Watts, R.L. and Koller, W.C. (eds), *Movement Disorders: Neurologic Principles and Practice*, McGraw-Hill, New York, pp. 503–523.
2. Huntington's Disease Collaborative Research Group (1993) A novel gene containing a trinucleotide repeat that is expanded and unstable on Huntington's disease chromosomes. *Cell*, **72**, 971–983.
3. Duyao, M.P., Auerbach, A.B., Ryan, A., Persichetti, F., Barnes, G.T., McNeil, S.M., Ge, P., Vonsattel, J.P., Gusella, J.F., Joyner, A.L. and MacDonald, M.E. (1995) Inactivation of the mouse Huntington's disease gene homolog Hdh. *Science*, **269**, 407–410.
4. Trushina, E., Dyer, R.B., Badger, J.D., Ure, D., Eide, L., Tran, D.D., Vrieze, B.T., Legendre-Guillemin, V., McPherson, P.S., Mandavilli, B.S. *et al.* (2004) Mutant huntingtin impairs axonal trafficking in mammalian neurons *in vivo* and *in vitro*. *Mol. Cell. Biol.*, **24**, 8195–8209.
5. Zhang, Y., Leavitt, B.R., van Raamsdonk, J.M., Dragatsis, I., Goldowitz, D., Macdonald, M.E., Hayden, M.R. and Friedlander, R.M. (2006) Huntingtin inhibits caspase-3 activation. *EMBO J.*, Epub ahead of print.
6. Cattaneo, E., Rigamonti, D., Goffredo, D., Zuccato, C., Squitieri, F. and Sipione, S. (2001) Loss of normal huntingtin function: new developments in Huntington's disease research. *Trends Neurosci.*, **24**, 182–188.
7. Ross, C.A., Wood, J.D., Schilling, G., Peters, M.F., Nucifora, F.C., Cooper, J.K., Sharp, A.H., Margolis, R.L. and Borchelt, D.R. (1999) Polyglutamine pathogenesis. *Phil. Trans. R. Soc. Lond. B. Biol. Sci.*, **354**, 1005–1011.
8. Mangiarini, L., Sathasivam, K., Seller, M., Cozens, B., Harper, A., Hetherington, C., Lawton, M., Trottier, Y., Lehrach, H., Davies, S.W. and Bates, G.P. (1996) Exon I of the HD gene with an expanded CAG repeat is sufficient to cause a progressive neurological phenotype in transgenic mice. *Cell*, **87**, 493–506.
9. Schilling, G., Becher, M.W., Sharp, A.H., Jinnah, H.A., Duan, K., Kotzuk, J.A., Slunt, H.H., Ratovitski, T., Cooper, J.K., Jenkins, N.A. *et al.* (1999) Intranuclear inclusions and neuritic aggregates in transgenic mice expressing a mutant N-terminal fragment of huntingtin. *Hum. Mol. Genet.*, **8**, 397–407.
10. Smith, K.M., Matson, S., Matson, W.R., Cormier, K., Del Signore, S.J., Hagerty, S.W., Stack, E.C., Ryu, H. and Ferrante, R.J. (2006) Dose ranging and efficacy study of high-dose coenzyme Q10 formulations in Huntington's disease mice. *Biochim. Biophys. Acta.*, **1762**, 616–626.
11. Stack, E.C., Kubilus, J.K., Smith, K., Cormier, K., Del Signore, S.J., Guelin, E., Ryu, H., Hersch, S.M. and Ferrante, R.J. (2005) Chronology of behavioral symptoms and neuropathological sequela in R6/2 Huntington's disease transgenic mice. *J. Comp. Neurol.*, **490**, 354–370.
12. Luthi-Carter, R., Hanson, S.A., Strand, A.D., Bergstrom, D.A., Chun, W., Peters, N.L., Woods, A.M., Chan, E.Y., Kooperberg, C., Krainc, D. *et al.* (2002) Dysregulation of gene expression in the R6/2 model of polyglutamine disease: parallel changes in muscle and brain. *Hum. Mol. Genet.*, **11**, 1911–1926.
13. Ryu, H. and Ferrante, R.J. (2005) Emerging chemotherapeutic strategies for Huntington's disease. *Expert Opin. Emerg. Drugs*, **10**, 345–363.
14. Sadri-Vakili, G. and Cha, J.H. (2006) Mechanisms of disease: histone modifications in Huntington's disease. *Nat. Clin. Pract. Neurol.*, **2**, 330–338.
15. Sugars, K.L. and Rubinsztein, D.C. (2003) Transcriptional abnormalities in Huntington disease. *Trends Genet.*, **19**, 233–238.
16. Hake, S.B., Xiao, A. and Allis, C.D. (2004) Linking the epigenetic 'language' of covalent histone modifications to cancer. *Br. J. Cancer*, **90**, 761–769.
17. Shogren-Knaak, M., Ishii, H., Sun, J.M., Pazin, M.J., Davie, J.R. and Peterson, C.L. (2006) Histone H4-K16 acetylation controls chromatin structure and protein interactions. *Science*, **311**, 844–847.
18. Ferrante, R.J., Kubilus, J.K., Lee, J., Ryu, H., Beesen, A., Zucker, B., Smith, K., Kowall, N.W., Ratan, R.R., Luthi-Carter, R. and Hersch, S.M. (2003) Histone deacetylase inhibition by sodium butyrate chemotherapy

ameliorates the neurodegenerative phenotype in Huntington's disease mice. *J. Neurosci.*, **23**, 9418–9127.
19. Gardian, G., Browne, S.E., Choi, D.K., Klivenyi, P., Gregorio, J., Kubilus, J.K., Ryu, H., Langley, B., Ratan, R.R., Ferrante, R.J. and Beal, M.F. (2005) Neuroprotective effects of phenylbutyrate in the N171–82Q transgenic mouse model of Huntington's disease. *J. Biol. Chem.*, **280**, 556–563.
20. Ferrante, R.J., Ryu, H., Kubilus, J.K., D'Mello, S., Sugars, K.L., Lee, J., Lu, P., Smith, K., Browne, S., Beal, M.F. *et al.* (2004) Chemotherapy for the brain: the antitumor antibiotic mithramycin prolongs survival in a mouse model of Huntington's disease. *J. Neurosci.*, **24**, 10335–10342.
21. Ryu, H., Lee, J., Hagerty, S.W., Soh, B.Y., McAlpin, S.E., Cormier, K., Smith, K.M. and Ferrante, R.J. (2006) ESET/SETDB1 gene expression and histone H3 (K9) trimethylation in Huntington's disease. *Proc. Natl Acad. Sci. USA*, **103**, 19176–19181.
22. Ferrante, R.J., Andreassen, O.A., Jenkins, B.G., Dedeoglu, A., Kuemmerle, S., Kubilus, J.K., Kaddurah-Daouk, R., Hersch, S.M. and Beal, M.F. (2000) Neuroprotective effects of creatine in a transgenic mouse model of Huntington's disease. *J. Neurosci.*, **20**, 4389–4397.
23. Murphy, K.P., Carter, R.J., Lione, L.A., Mangiarini, L., Mahal, A., Bates, G.P., Dunnett, S.B. and Morton, A.J. (2000) Abnormal synaptic plasticity and impaired spatial cognition in mice transgenic for exon 1 of the human Huntington's disease mutation. *J. Neurosci.*, **20**, 5115–5123.
24. Bogdanov, M.B., Andreassen, O.A., Dedeoglu, A., Ferrante, R.J. and Beal, M.F. (2001) Increased oxidative damage to DNA in a transgenic mouse model of Huntington's disease. *J. Neurochem.*, **79**, 1246–1249.
25. Hersch, S.M., Gevorkian, S., Marder, K., Moskowitz, C., Feigin, A., Cox, M., Como, P., Zimmerman, C., Lin, M., Zhang, L. *et al.* (2006) Creatine in Huntington disease is safe, tolerable, bioavailable in brain and reduces serum 8OH2′dG. *Neurology*, **66**, 250–252.
26. Bannister, A.J., Schneider, R. and Kouzarides, T. (2002) Histone methylation: dynamic or static? *Cell*, **109**, 801–806.
27. Felsenfeld, G. and Groudine, M. (2003) Controlling the double helix. *Nature*, **421**, 448–453.
28. Lee, D.Y., Hayes, J.J., Pruss, D. and Wolffe, A.P. (1993) A positive role for histone acetylation in transcription factor access to nucleosomal DNA. *Cell*, **72**, 73–84.
29. Strahl, B.D. and Allis, C.D. (2000) The language of covalent histone modifications. *Nature*, **403**, 41–45.
30. Hake, S.B. and Allis, C.D. (2006) Histone H3 variants and their potential role in indexing mammalian genomes: the 'H3 barcode hypothesis'. *Proc. Natl Acad. Sci. USA*, **103**, 6428–6435.
31. Papp, B. and Müller, J. (2006) Histone trimethylation and the maintainence of transcriptional ON and OFF states by trxG and PcG proteins. *Genes Dev.*, **20**, 2041–2054.
32. Mattson, M.P. and Sherman, M. (2003) Perturbed signal transduction in neurodegenerative disorders involving aberrant protein aggregation. *Neuromolecular Med.*, **4**, 109–132.
33. Robakis, N.K. (2003) An Alzheimer's disease hypothesis based on transcriptional dysregulation. *Amyloid*, **10**, 80–85.
34. Kim, H.S., Kim, E.M., Kim, N.J., Chang, K.A., Choi, Y., Ahn, K.W., Lee, J.H., Kim, S., Park, C.H. and Suh, Y.H. (2004) Inhibition of histone deacetylation enhances the neurotoxicity induced by the C-terminal fragments of amyloid precursor protein. *J. Neurosci. Res.*, **75**, 117–124.
35. Mandel, S., Grunblatt, E., Riederer, P., Amariglio, N., Jacob-Hirsch, J., Rechavi, G. and Youdim, M.B. (2005) Gene expression profiling of sporadic Parkinson's disease substantia nigra pars compacta reveals impairment of ubiquitin-proteasome subunits, SKP1A, aldehyde dehydrogenase, and chaperone HSC-70. *Ann. NY Acad. Sci.*, **1053**, 356–375.
36. Luthi-Carter, R., Strand, A., Peters, N.L., Solano, S.M., Hollingsworth, Z.R., Menon, A.S., Frey, A.S., Spektor, B.S., Penney, E.B., Schilling, G. *et al.* (2000) Decreased expression of striatal signaling genes in a mouse model of Huntington's disease. *Hum. Mol. Genet.*, **9**, 1259–1271.
37. Zhai, W., Jeong, H., Cui, L., Krainc, D. and Tjian, R. (2005) *In vitro* analysis of huntingtin-mediated transcriptional repression reveals multiple transcription factor targets. *Cell*, **123**, 1241–1253.
38. Bianchi, N., Passadore, M., Rutigliano, C., Feriotto, G., Mischiati, C. and Gambari, R. (1996) Targeting of the Sp1 binding sites of HIV-1 long terminal repeat with chromomycin. Disruption of nuclear factor. DNA complexes and inhibition of *in vitro* transcription. *Biochem. Pharmacol.*, **52**, 1489–1498.
39. Chiang, S.Y., Welch, J.J., Rauscher, F.J. and Beerman, T.A. (1996) Effect of DNA-binding drugs on early growth response factor-1 and TATA box-binding protein complex formation with the herpes simplex virus latency promoter. *J. Biol. Chem.*, **271**, 23999–24004.
40. Welch, J.J., Rauscher, F.J. and Beerman, T.A. (1994) Targeting DNA-binding drugs to sequence-specific transcription factor DNA complexes. Differential effects of intercalating and minor groove binding drugs. *J. Biol. Chem.*, **269**, 31051–31058.
41. White, C.M., Heidenreich, O., Nordheim, A. and Beerman, T.A. (2000) Evaluation of the effectiveness of DNA-binding drugs to inhibit transcription using the c-fos serum response element as a target. *Biochemistry*, **39**, 12262–12273.
42. Mir, M.A., Majee, S., Das, S. and Dasgupta, D. (2003) Association of chromatin with anticancer antibiotics, mithramycin and chromomycin A3. *Bioorg. Med. Chem.*, **11**, 2791–2801.
43. Chakrabarti, S., Bhattacharyya, D. and Dasgupta, D. (2001) Structural basis of DNA recognition by anticancer antibiotics, chromomycin A(3), and mithramycin: roles of minor groove width and ligand flexibility. *Biopolymers*, **56**, 85–95.
44. Rabbani, A., Finn, R.M. and Ausio, J. (2004) The anthracycline antibiotics: antitumor drugs that alter chromatin structure. *Bioessays*, **27**, 50–56.
45. Sastry, M., Fiala, R. and Patel, D.J. (1995) Solution structure of mithramycin dimers bound to partially overlapping sites on DNA. *J. Mol. Biol.*, **251**, 674–689.
46. Rabbani, A., Finn, R.M., Thambirajah, A.A. and Ausio, J. (2004) Binding of antitumor antibiotic daunomycin to histones in chromatin and solution. *Biochemistry*, **43**, 16497–16504.
47. Yamamoto, A., Lucas, J.J. and Hen, R. (2000) Reversal of neuropathology and motor dysfunction in a conditional model of Huntington's disease. *Cell*, **101**, 57–66.
48. Jenuwein, T. and Allis, C.D. (2001) Translating the histone code. *Science*, **293**, 1074–1080.
49. Ralston, S.H. (1994) Pathogenesis and management of cancer associated hypercalcaemia. *Cancer Surv.*, **21**, 179–196.
50. Ryan, W.G. (1974) Treatment of Paget's disease of bone with mithramycin. *Clin. Orthop.*, **127**, 106–110.
51. Kennedy, B.J. (1972) Mithramycin therapy in testicular cancer. *Urology*, **107**, 429–432.
52. Krapf, H., Morrissey, S.P., Zenker, O., Zwingers, T., Gonsette, R., Hartung, H.P. and MIMS Study Group (2005) Effect of mitoxantrone on MRI in progressive MS: results of the MIMS trial. *Neurology*, **65**, 690–695.
53. Schimmel, K.J., Richel, D.J., van den Brink, R.B. and Guchelaar, H.J. (2004) Cardiotoxicity of cytotoxic drugs. *Cancer Treat. Rev.*, **30**, 181–191.
54. Bolstad, B.M., Collin, F., Brettschneider, J., Cope, L., Simpson, K., Irizarry, R.A. and Speed, T.P. (2005) Quality assessment of affymetrix genechip data. In Gentleman, R., Carey, V., Huber, W., Irizarry, R. and Dudoit, S. (eds), *Bioinformatics and Computational Biology Solutions Using R and Bioconductor*, Springer, New York, pp. 33–48.
55. Franklin, K.B.J. and Paxinos, G. (2000) *The Mouse Brain in Stereotactic Coordinates*. Academic Press, New York.
56. Rasband, W.S. (1997–2006) *Image J*. U.S. National Institutes of Health, Bethesda, MD, USA, http://rsb.info.nih.gov/ij/://rsb.info.nih.gov/ij/.
57. Bogdanov, M.B., Beal, M.F., McCabe, D.R., Griffin, R.M. and Matson, W.R. (1999) A carbon column-based liquid chromatography electrochemical approach to routine 8-hydroxy-2′-deoxyguanosine measurements in urine and other biologic matrices: a one-year evaluation of methods. *Free Radic. Biol. Med.*, **27**, 647–666.
58. Bolstad, B.M., Irizarry, R.A., Astrand, M. and Speed, T.P. (2003) A comparison of normalization methods for high density oligonucleotide array data based on bias and variance. *Bioinformatics*, **19**, 185–193.
59. Irizarry, R.A., Bolstad, B.M., Collin, F., Cope, L.M., Hobbs, B. and Speed, T.P. (2003) Summaries of Affymetrix GeneChip probe level data. *Nucleic Acids Res.*, **31**, e15.
60. Gautier, L., Cope, L., Bolstad, B.M. and Irizarry, R.A. (2004) affy—analysis of Affymetrix GeneChip data at the probe level. *Bioinformatics*, **203**, 307–315.
61. Lönnstedt, I. and Speed, T.P. (2002) Replicated microarray data. *Stat. Sin.*, **12**, 31–46.
62. Smyth, G.K. (2004) Linear models and empirical Bayes methods for assessing differential expression in microarray experiments. *Stat. Appl. Genet. Mol. Biol.*, **3**, Article 3.